Plant Physiology and Biochemistry 142 (2019) 34–42

Contents lists available at ScienceDirect

Plant Physiology and Biochemistry

journal homepage: www.elsevier.com/locate/plaphy

Research article

Expression of the p24 silencing suppressor of *Grapevine leafroll-associated virus 2* from *Potato virus X* or *Barley stripe mosaic virus* vector elicits hypersensitive responses in *Nicotiana benthamiana*

Xianyou Wang[a,b], Chen Luo[a,b], Yanfei Xu[c], Chenwei Zhang[a,b], Mian Bao[a,b], Junjie Dou[a,b], Qi Wang[d], Yuqin Cheng[a,b,*]

[a] Department of Pomology, China Agricultural University, Beijing, 100193, China
[b] Key Laboratory of Viticulture and Enology, Ministry of Agriculture, Beijing, 100083, China
[c] DeLaval Tianjin Company, Tianjin, 300308, China
[d] Department of Plant Pathology, China Agricultural University, Beijing, 100193, China

ARTICLE INFO

Keywords:
p24
Grapevine leafroll-Associated virus 2
RNA-Silencing suppressor
Pathogenicity
Hypersensitive response

ABSTRACT

The 24-kDa protein (p24) encoded by *Grapevine leafroll-associated virus 2* (GLRaV-2) is an RNA-silencing suppressor (RSS), but its effect on active viral infection is unclear. Using a *Potato virus X* (PVX)-based expression system, we demonstrated that p24 elicits lethal systemic necrosis in *Nicotiana benthamiana*, sharing typical characteristics of the hypersensitive response (HR), and that NbRAR1 (a cytoplasmic Zn^{2+}-binding protein) is involved in the PVX–p24-mediated systemic necrosis. Moreover, expression of p24 from *Barley stripe mosaic virus* (BSMV) vector triggered local necrosis in infiltrated patches of *N. benthamiana*, likely inhibiting viral systemic spread. By deletion analysis, we demonstrated that amino acids (aa) 1 to 180, which are located in the region (aa 1–188) previously shown to be necessary for p24's RSS activity, is sufficient for p24 to elicit systemic necrosis in the context of PVX infection. Using substitution mutants, we revealed that silencing-suppression-defective mutants R2A and W54A induce only a mild necrotic response; two mutants without self-interaction ability previously shown to lose or retain weak suppression function also displayed decreased pathogenicity: W149A without RSS activity elicited a mild necrotic response, whereas V162H/L169H/L170H which retains weak RSS activity was able to induce systemic necrosis, but with a 1- to 2-day delay. Taken together, p24 plays an important role in GLRaV-2 pathogenesis, triggering HR-like necrosis in *N. benthamiana* plants when expressed from PVX or BSMV vector; both the silencing suppression and self-interaction are crucial for p24's pathogenicity activity, and the region of p24 for determining systemic necrosis is mapped to aa 1–180.

1. Introduction

Post-transcriptional gene silencing plays a critical role in plant resistance to viruses. As a counter-defensive strategy, most plant viruses have evolved RNA-silencing suppressors (RSSs). Viral RSSs can cause developmental abnormalities by interfering with the function of microRNAs, thus resembling disease symptoms (reviewed in Wang et al., 2012). Given the importance of suppressing RNA silencing for virus survival, viral RSSs can be elicitors of resistance (*R*) gene-driven effector triggered immunity (ETI) causing hypersensitive response (HR) (reviewed in García and Pallás, 2015). Mixed viral infection of plant viruses may lead to more severe symptoms than individual viral components (a phenomenon called viral synergism). Since viral RSSs help to overcome RNA silencing mechanisms of hosts, it is not unexpected that they are responsible for disease synergism (Pruss et al., 1997; Cuellar et al., 2009; Siddiqui et al., 2011). Similarly, co-expression of other viral RNA silencing suppressors enhances *Potato virus X* (PVX) virulence. For example, heterologous expression of *Tomato bushy stunt virus* (TBSV) p19 (Scholthof et al., 1995; Angel and Schoelz, 2013), V2 protein of monopartite begomovirus (Mubin et al., 2010), and p23 protein of *Citrus tristeza virus* (CTV) (Ruiz-Ruiz et al., 2013) from PVX vector induced a dramatic enhancement of the disease symptoms caused by PVX, resulting in systemic necrosis and eventually plant death. Thus, viral RSSs generally play important roles for viral pathogenicity.

HR is a type of programmed cell death that localizes the virus to the primary infection site, and NbRar1 is required for HR induction (Liu et al., 2002). Systemic necrosis, one of the most severe symptoms in

* Corresponding author. Department of Pomology, China Agricultural University, Beijing, 100193, China.
E-mail address: chengyuqin@cau.edu.cn (Y. Cheng).

https://doi.org/10.1016/j.plaphy.2019.06.033
Received 8 March 2019; Received in revised form 24 May 2019; Accepted 23 June 2019
Available online 25 June 2019

susceptible plants that eventually results in plant death, shares remarkable similarities with HR: both involve programmed cell death, altered expression of similar defense-related genes, and triggered reactive oxygen species accumulation; and it is suggested that systemic necrosis is merely an uncontrolled or incomplete HR-associated necrosis response that is triggered in distal tissues when the localized HR fails to limit virus spread (reviewed in Mandadi and Scholthof, 2013).

Grapevine leafroll disease is a globally distributed virus disease, and *Grapevine leafroll-associated virus 2* (GLRaV-2) is considered to be one of the prevalent GLRaVs in leafroll-affected grapevines (Naidu et al., 2015). In natural conditions, GLRaV-2 mostly infects grapevine but can be transmitted experimentally to some *Nicotiana* species inducing obvious symptoms (Goszczynski et al., 1996; Ghanem-Sabanadzovic et al., 2000). For example, GLRaV-2 isolate '94/970' can systemically infect *N. benthamiana* plants via mechanical transmission, and infected plants display symptoms of chlorotic local lesions, resulting in stem necrosis and death of the plant (Goszczynski et al., 1996). This isolate is virtually identical to isolates 'PN' (GenBank Acc. No. AF039204) and 'Sem' (Meng et al., 2005). Ghanem-Sabanadzovic et al. (2000) also reported that GLRaV-2 isolate H4 can invade systemically *N. benthamiana* inducing systemic vein clearing and curing of the leaves and *N. occidentalis* in which it elicits necrotic local lesions followed by apical necrosis and death of the plants. GLRaV-2 is a member of the genus *Closterovirus* in the family *Closteroviridae*. The genome of GLRaV-2 encompasses nine open reading frames (ORFs). ORFs 1a and 1b encode a polyprotein (Liu et al., 2009). ORFs 2–7 encode small hydrophobic protein 6, heat-shock 70 protein homolog (HSP70h), 63-kDa protein, minor capsid protein (CPm), CP, 19-kDa protein and p24 (Liu et al., 2009). GLRaV-2 p24 is an RSS (Chiba et al., 2006; Li et al., 2018), while its biological function remains largely unclear.

In the present study, we demonstrated that expression of GLRaV-2 p24 from PVX or BSMV vector elicits HR-like necrosis in *N. benthamiana* plants, and *NbRAR1* contributes to the necrotic response. Using deletion and substitution mutants, we identified the functional region of p24 required for PVX–p24-induced systemic necrosis and showed that the silencing suppression and self-interaction are both crucial for p24's pathogenic activity.

2. Materials and methods

2.1. Plant material

N. benthamiana plants and 'Cabernet Sauvignon' in vitro-grown grapevine plantlets were grown under controlled conditions at 25 °C with a 16-h light regime.

2.2. Construction of recombinant PVX vectors

The primer sequences are given in Table S1. The p24 protein here is the same one used in our previous studies (Liu et al., 2016a; Li et al., 2018), and the sequence of *p24* (MK894576) was previously amplified from RNA extracted from 'Cabernet Sauvignon' in vitro-grown grapevine plantlets naturally infected with GLRaV-2 isolate SD by RT-PCR method. In this study, pGD–p24 (Li et al., 2018) was used to amplified sequences of p24, p24 (1–188), p24 (1–180), p24 (1–170), p24 (1–160), p24 (1–150), p24 (1–130), p24 (1–100), p24 (1–80), p24 (10–188), p24 (10–180), and R2A using primer pairs F1/R1, F1/R2, F1/R3, F1/R4, F1/R5, F1/R6, F1/R7, F1/R8, F1/R9, F2/R2, F2/R3, and F3/R1, respectively. For deletion analysis of p24 protein, start and/or stop codons were added.

Primer pairs F4/R10, F5/R11, F6/R12, and F7/R13 were used for amplifying sequences of *RdRP*, *HSP70h*, *CPm*, and *CP*, respectively. Total RNA was extracted from the in vitro-grown grapevine plantlets described above using the RNeasy Plant Mini kit (Qiagen). Synthesis of cDNA (at temperature 42°C) was primed with a mix of random primers and oligo dT provided by SYBR® PrimeScript™ RT-PCR Kit (TaKaRa) using 500 ng of total RNA.

The templates for amplification of the substitution mutants I35H, W54A, W149A, and V162H/L169H/L170H were pGD–35H, pGD–54A, pGD–149A, and pGD–162/169/170H (Li et al., 2018), respectively, and the primer pair was F1/R1.

PCR amplification was conducted as follows: cDNA denaturation at 94 °C for 5 min; 35 cycles at 94 °C for 30 s, 60–65 °C (depending on the specific primer pair used) for 30 s and 72 °C for 30 s to 1 min 50 s (depending on the specific primer pair used), and a final extension step at 72 °C for 10 min. PCR analysis was conducted in a thermalcycler (T100™ from Bio-Rad). The PCR products were digested with *Cla*I/*Sal*I, and cloned into the PVX vector (Chapman et al., 1992) according to the method previously described (Mubin et al., 2010).

2.3. Agroinfection

PVX and the recombinant PVX vectors were transformed into *Agrobacterium tumefaciens* strain GV3101. Young, fully expanded leaves of 4-week-old *N. benthamiana* plants were used for agroinfection. Agroinfection was performed as described previously (Mubin et al., 2010).

2.4. Expression of p24 from BSMV vector in N. benthamiana

BSMV vector (Lawrence and Jackson, 2001) consisted of pCaBS-α, pCaBS-β and pCaBS-γ plasmids comprising, respectively, the tripartite genome (RNAα, RNAβ, and RNAγ). The recombinant vector BSMV–p24 was created as previously described (Tai et al., 2007). Briefly, the sequence of *p24* was amplified with primer pair F13/R19. PCR amplification was conducted as follows: cDNA denaturation at 94 °C for 5 min; 35 cycles at 94 °C for 30 s, 62 °C for 30 s and 72 °C for 30 s, and a final extension step at 72 °C for 10 min. PCR products were digested with *Mlu*I/*Apa*I, and cloned into pCaBS-γ to produce pCaBS-γ–p24. The combination of pCaBS-α, pCaBS-β and pCaBS-γ–p24 was named BSMV–p24.

A. tumefaciens strain EHA105 carrying pCaBS-α, pCaBS-β, pCaBS-γ or pCaBS-γ–p24 was cultured separately and agroinfiltration was performed as described previously (Mubin et al., 2010).

2.5. Cell death analysis and hydrogen peroxide (H_2O_2) detection

Trypan blue and 3, 3′-diaminobenzidine (DAB) staining were performed essentially as described previously (Liu et al., 2016b). The experiments were conducted independently three times.

2.6. RT-PCR detection and real-time quantitative RT-PCR (qRT-PCR)

The primer pairs F16/R22 and F13/R19 were used for RT-PCR detection of BSMV CP and GLRaV-2 p24, respectively. The PCR program consisted of 5 min at 95 °C, followed by 35 cycles of 95 °C for 30 s, 58 °C (for CP) or 62 °C (for p24) for 30 s, and 72 °C for 45 s. This was followed by a final extension for 10 min at 72 °C.

qRT-PCR was performed with SYBR® PrimeScript™ RT-PCR Kit according to the manufacturer's instructions. The relative expression levels of PVX *CP*, *NbPR1* (JN247448.1), *NbPR10* (KF841443.1), and *NbRAR1* (LC314308.1) were analyzed using primer pairs F12/R18, F9/R15, F10/R16, and F15/R21 (Table S1), respectively. *N. benthamiana GAPDH* was analyzed as an internal control using primer pair F11/R17. qPCR analysis was conducted in an ABI 7500 thermocycler (Applied Biosystems, Foster City, CA, USA). Quantification was conducted according to a previously described method (Pfaffl, 2001).

2.7. Virus-induced gene silencing (VIGS) treatment

VIGS vectors derived from *Tobacco rattle virus* (TRV) consisted of pTRV1 and pTRV2 (Liu et al., 2002). Construction of VIGS vector was

performed as described previously (Komatsu et al., 2010). Briefly, a 336-bp PCR fragment corresponding to *NbRAR1* was amplified from total RNA extracted from *N. benthamiana* leaves by RT-PCR using primer pair F14/R20. The PCR program consisted of 5 min at 95 °C, followed by 35 cycles of 95 °C for 30 s, 58 °C for 30 s, 72 °C for 45 s, and a final extension step at 72 °C for 10 min. PCR products were digested with *SmaI/BamH*I, and cloned into pTRV2 to produce pTRV2–RAR1. The combination of pTRV1 and pTRV2–RAR1 was named TRV–RAR1. pTRV1, pTRV2 and its derivative pTRV2–RAR1 were respectively transformed into *A. tumefaciens* strain GV3101. Agroinfiltration was performed as described previously (Mubin et al., 2010).

Silencing of *NbRAR1* mRNA was detected from the first upper noninfiltrated leaves by qRT-PCR using the primer pair F15/R21 at 15 days after induction of *NbRAR1* silencing. The experiments were conducted independently three times.

2.8. Protein extraction and western analysis

N. benthamiana leaves were ground in liquid nitrogen and mixed with 2 × SDS sample buffer containing 10% (v/v) β-mercaptoethanol. The samples were then boiled at 100 °C for 5 min, and centrifuged for 5 min at 13,000*g* before loading on a gel. Proteins were separated by 12% SDS-PAGE and Western blot analysis was performed by probing first with rabbit anti-p24 antiserum (diluted 1:2000) (non-commercial antibody) to detect GLRaV-2 p24 and its mutants, or rabbit anti-PVX CP antiserum (diluted 1:5000) (non-commercial antibody, kindly provided by Dr C.-G. Han, China Agricultural University, Beijing, China) to detect PVX CP, followed by alkaline phosphatase–goat anti-rabbit IgG (1:5,000, Bio-Rad). Finally, GLRaV-2 p24 and PVX CP was detected with the substrates 5-bromo-4-chloro-3-indolyl phosphate/nitroblue tetrazolium (Sigma). An equal amount of protein content for each lane was verified by Coomassie brilliant blue staining.

3. Results

3.1. GLRaV-2 p24 elicits necrosis in N. benthamiana when expressed from PVX or BSMV vector

We expressed five selected proteins (RdRP, HSP70h, CP, CPm and p24) of GLRaV-2 using a PVX-based expression assay to analyze their role in viral pathogenicity. The recombinant viruses PVX–CP, PVX–HSP70h, PVX–RdRP, PVX–CPm and PVX–p24 were respectively infiltrated into leaves of *N. benthamiana* plants. Infiltration of PVX with no insert was used as a control. Three independent experiments were carried out, and symptom development on the agroinfiltrated plants was monitored daily. The results of the agroinfiltration of plants with the above constructs are summarized in Table 1.

As shown in Fig. 1A, plants infiltrated with PVX–CP or PVX–RdRP showed mild mosaic symptoms, similar to that of plants infected with PVX, whereas the majority of plants infiltrated with PVX–CPm or PVX–HSP70h showed enhanced systemic mosaic symptoms with a few necrotic spots on the first two systemically infected leaves at 10–12 days postinfiltration (dpi); these symptoms never developed, but persisted for several weeks after infiltration. However, expression of p24 elicited lethal systemic necrosis: leaves infiltrated with PVX–p24 developed local lesions at the site of inoculation at 4 dpi; at 8 dpi, the plants showed typical apical necrosis that ultimately led to the death of the entire plant at 12 dpi. We observed that RdRP, HSP70h, CP, CPm and p24 genes are all accurately maintained in the viral progeny detected by RT-PCR (data not shown).

Exacerbation of the symptoms produced by recombinant PVX viruses expressing viral RSSs has been reported to be linked to an increase in the accumulation of PVX RNA in infected plants (Deng et al., 2015; Fujita et al., 2018). We analyzed the accumulation of PVX CP in infiltrated leaves at 3 dpi, and in the first systemically infected and upper young leaves of PVX–p24-infected plants that did not show necrosis at 4, 5 and 6 dpi by western blotting. PVX viral RNA in the first systemically infected leaves at 5 dpi, and in the upper young leaves at 4 and 5 dpi was also detected by qRT-PCR. The qRT-PCR results showed a significantly lower level of PVX RNA in PVX–p24-infected plants than in their PVX-infected counterparts (Fig. 1 B). Western blotting showed that accumulation of PVX CP in the infiltrated and upper young leaves was obviously lower in PVX–p24-infected plants (Fig. 1C, lanes 2, 10, 12, 14) than in PVX-infected plants (Fig. 1C, lanes 1, 9, 11, 13); there were no major differences in the first systemically leaves of PVX–p24- (Fig. 1C, lanes 3, 5, 7) and PVX-infected (Fig. 1C, lanes 4, 6, 8) plants at 4, 5 and 6 dpi. These results indicated that the severe symptoms in the presence of p24 are not a consequence of increasing accumulation of PVX.

Since RdRP, HSP70h, CP, and CPm have little or no effect on viral pathogenicity, they were not further analyzed in this study. To further investigate the role of p24 in pathogenesis, the *p24* sequence was cloned into the BSMV vector to generate the recombinant plasmid BSMV–p24. Leaves of 4-week-old *N. benthamiana* plants were agroinfiltrated with BSMV–p24, or with BSMV as a control. Local necrosis was observed in the infiltrated patches of all BSMV–p24-infiltrated plants at 9–10 dpi, while the upper noninfiltrated leaves were symptomless (Fig. 1A), and remained symptomless for several weeks (data not shown). In contrast, no necrotic response was observed in any of the BSMV-infiltrated plants (Fig. 1A). Identical results were obtained in

Table 1
Summary of agroinfiltration in three independent experiments.

Construct	Phenotype	Plants exhibited phenotype/total plants
PVX–HSP70h	Enhanced mosaic symptoms with a mild necrotic response	5/7, 5/6, 6/7
PVX–CP	Mild mosaic symptoms	7/7, 6/6, 7/7
PVX–RdRP	Mild mosaic symptoms	6/6, 4/4, 5/5
PVX–CPm	Enhanced mosaic symptoms with a mild necrotic response	4/6, 4/5, 4/5
PVX	Mild mosaic symptoms	6/7, 8/8, 6/6
PVX–p24	Lethal systemic necrosis	10/10, 13/13, 12/12
BSMV–p24	Local lesions at the site of inoculation	9/9, 8/8, 8/8
BSMV	No obvious symptoms	7/7, 7/7, 6/6
PVX–p24 (1–188)	Lethal systemic necrosis	6/6, 7/7, 5/5
PVX–p24 (1–180)	Lethal systemic necrosis	8/8, 7/7, 5/5
PVX–p24 (1–170)	Enhanced mosaic symptoms with a mild necrotic response	6/6, 6/7, 7/7
PVX–p24 (1–160)	Enhanced mosaic symptoms with a mild necrotic response	6/6, 6/6, 6/6
PVX–p24 (1–150)	Enhanced mosaic symptoms with a mild necrotic response	7/7, 5/5, 5/5
PVX–p24 (1–130)	Enhanced mosaic symptoms with a mild necrotic response	7/7, 7/7, 5/5
PVX–p24 (1–100)	No necrotic response	7/7, 6/6, 6/6
PVX–p24 (1–80)	No necrotic response	6/6, 7/7, 5/5
PVX–p24 (10–180)	Mild mosaic symptoms	9/9, 8/8, 7/7
PVX–p24 (10–188)	Enhanced mosaic symptoms with a mild necrotic response	8/8, 8/8, 6/6

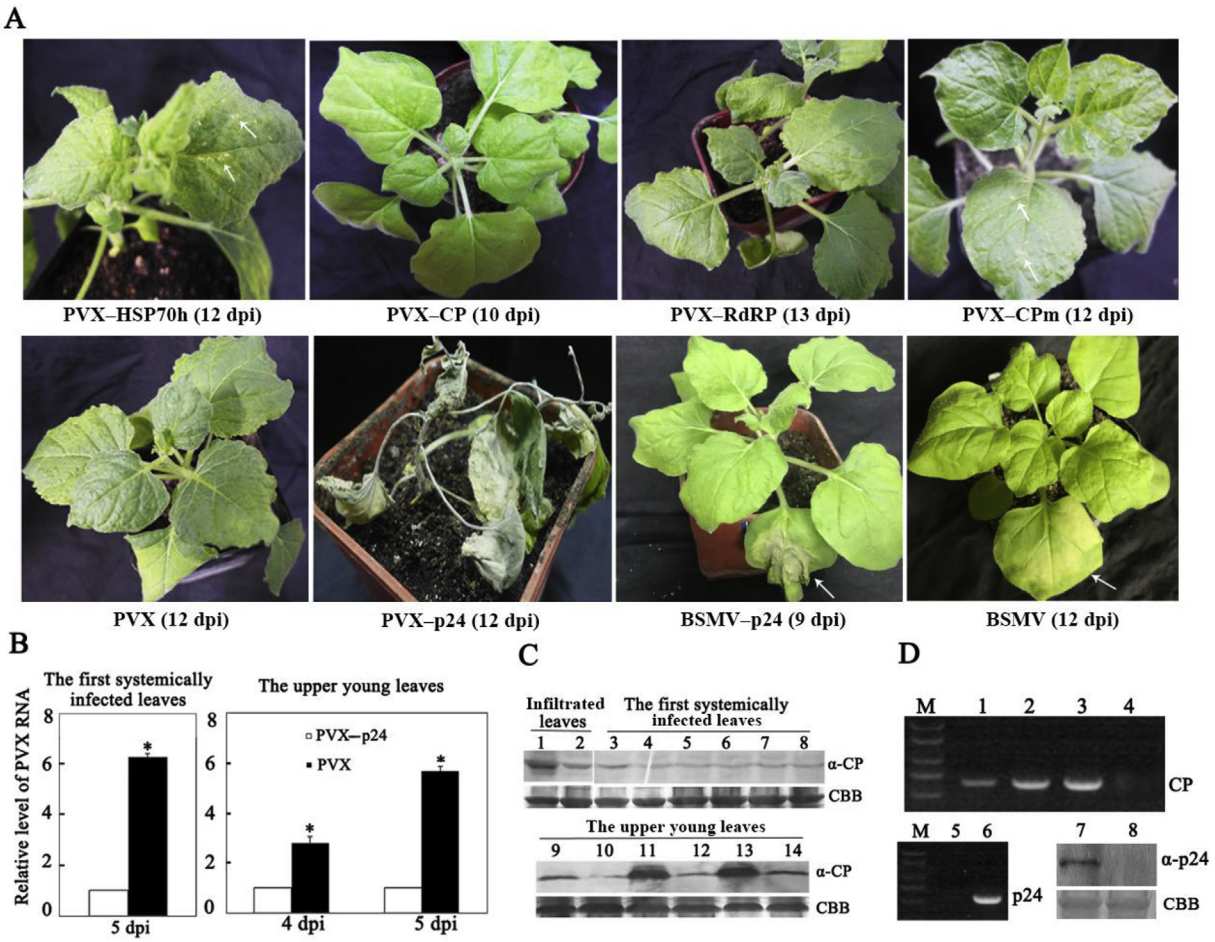

Fig. 1. GLRaV-2 p24 elicits necrosis in *N. benthamiana* when expressed from PVX or BSMV vector. (A) Phenotypes of *N. benthamiana* induced by GLRaV-2 proteins expressed from PVX or p24 expressed from BSMV vector. Arrows indicate necrotic spots (upper panel) and infiltrated leaves (lower panel). (B) Quantitative assessment of PVX RNA accumulation. qRT-PCR results are shown as the mean ± SD of three independent experiments. SD is denoted by the error bars. *P < 0.05. (C) Quantitative assessment of PVX CP accumulation using PVX CP-specific antiserum. Total proteins were extracted from the infiltrated leaves at 3 dpi, the first systemically infected leaves and the upper young leaves at 4 dpi (lanes 3, 4, and 9, 10), 5 dpi (5, 6, and 11, 12), and 6 dpi (7, 8, and 13, 14). Odd and even numbers indicate samples from PVX- and PVX–p24-infected plants, respectively. CBB: Coomassie brilliant blue staining served as loading control. (D) Detection of BSMV CP and GLRaV-2 p24 genes and p24 expression (lower right panel). Lane 1–2: BSMV infiltrated and upper noninfiltrated leaves, respectively. BSMV–p24 infiltrated (lanes 3, 6, 7) and upper noninfiltrated (lanes 4, 5, 8) leaves. The infiltrated and upper noninfiltrated leaves were harvested at 7 and 10 dpi, respectively. M: DNA marker. (For interpretation of the references to color in this figure legend, the reader is referred to the Web version of this article.)

three independent experiments.

To detect BSMV infection and the GLRaV-2 p24 gene in the viral progeny, we performed RT-PCR to amplify the sequence of BSMV *CP* and GLRaV-2 *p24* in infiltrated leaves at 7 dpi and in the upper non-infiltrated leaves at 10 dpi. BSMV CP (Fig. 1D, lane 3) and p24 (Fig. 1D, lane 6) genes both were detected in the BSMV–p24-infiltrated tissues, but not in the upper noninfiltrated leaves of the plants (Fig. 1D, lanes 4, 5). Western blotting using an anti-p24 antiserum also substantiated the results seen with RT-PCR: p24 expression was detected in the BSMV–p24-infiltrated leaves at 7 dpi (Fig. 1D, lane 7), but not in the upper noninfiltrated leaves at 10 dpi (Fig. 1D, lane 8). In contrast, BSMV CP gene was detected in both infiltrated tissues and upper non-infiltrated leaves of BSMV-infected plants (Fig. 1D, lanes 1, 2). These results indicated that the expression of p24 from BSMV vector elicits HR-like necrosis, which may restrict systemic spread of the recombinant BSMV–p24.

Together, our results indicated that heterologous expression of p24 from PVX or BSMV vector significantly enhances disease symptoms caused by PVX or BSMV, suggesting the important role of p24 in viral pathogenesis.

3.2. Systemic necrosis elicited by PVX–p24 in N. benthamiana is associated with HR characteristics

To investigate whether systemic necrosis induced by PVX–p24 is accompanied by biochemical features and gene-expression patterns that are characteristic of the HRs, cell death, accumulation of H_2O_2, and induction of defense-related genes were examined. The upper PVX–p24-infected leaves of *N. benthamiana* plants were treated with trypan blue at 6 dpi. Trypan blue is used to selectively stain dead cells. PVX–p24-infected leaves were deeply stained, while the PVX-infected leaves were only lightly stained (Fig. 2A). These results confirmed the occurrence of cell death in response to p24 expression from PVX vector.

The upper noninfiltrated leaves of PVX- and PVX–p24-infected plants at 6 dpi were analyzed by DAB staining. In the presence of H_2O_2, DAB polymerizes to produce a deep brown color that can be visualized after ethanol clearing of the tissue. PVX–p24-infected leaves accumulated high concentrations of H_2O_2 (Fig. 2B).

Pathogenesis-related (PR) genes *PR1* and *PR10* are involved in viral infection (Liu et al., 2017). The transcript levels of *NbPR1* and *NbPR10* in the first systemically infected leaves at 5 dpi, and the upper young leaves at 4 and 5 dpi, before necrosis, were investigated by qRT-PCR. *NbPR1* was significantly elevated in the PVX–p24-infected plants at 5

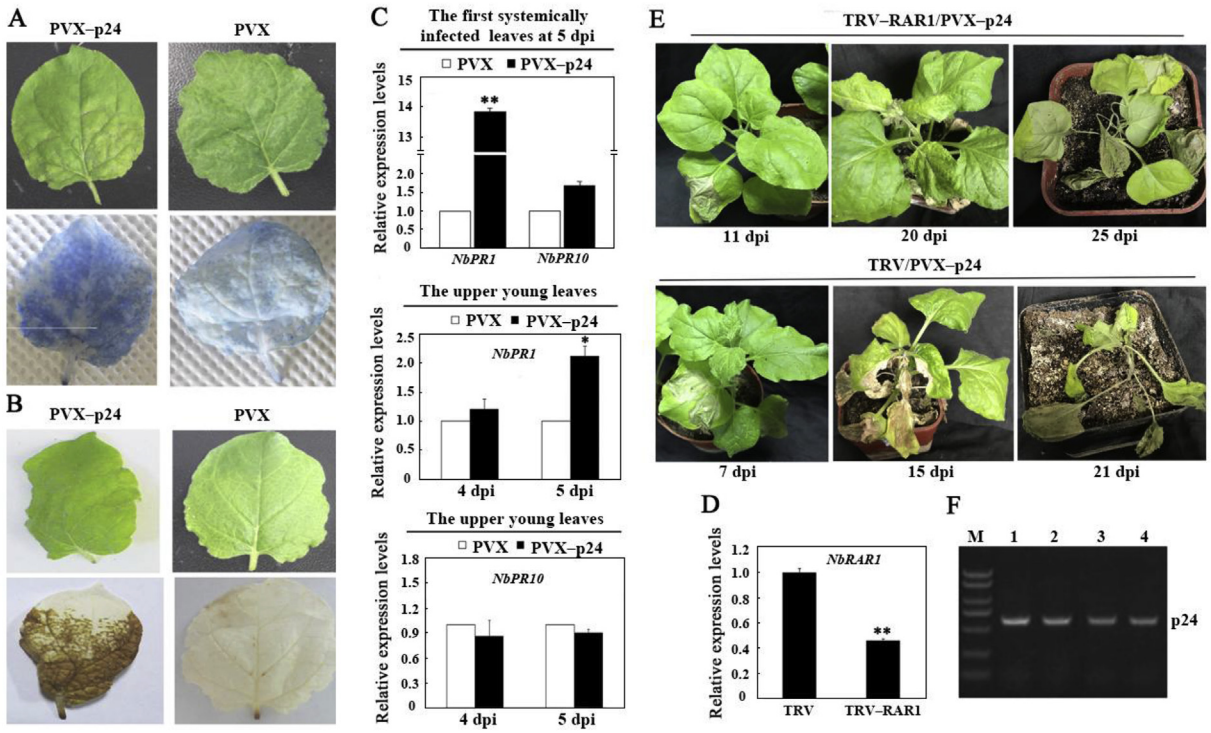

Fig. 2. Systemic necrosis induced by PVX–p24 has HR characteristics and *NbRAR1* is involved in the necrotic response. (A) Trypan blue staining. (B) Assessment of H_2O_2 accumulation by DAB staining. (C) The expression of *NbPR1* and *NbPR10*. (D) Confirmation of *NbRAR1* silencing by qRT-PCR. (E) *NbRAR1* silencing results in the delay of PVX–p24-mediated necrotic response. (F) Detection of p24 gene in the infiltrated and upper noninfiltrated leaves of TRV/PVX–p24-infected (lanes 1, 2) and TRV–RAR1/PVX–p24-infected (lanes 3, 4) plants. M: DNA marker. (For interpretation of the references to color in this figure legend, the reader is referred to the Web version of this article.)

dpi, whereas no major change was observed in the expression level of *NbPR10* (Fig. 2C).

These results revealed that systemic necrosis induced by PVX–p24 is associated with cell death, accumulation of H_2O_2, and induction of *NbPR1*.

3.3. NbRAR1 is involved in the systemic necrosis elicited by PVX–p24

NbRAR1 plays an essential role in R-gene-mediated HR (Liu et al., 2002; Muskett et al., 2002). To investigate whether NbRAR1 is involved in the induction of systemic necrosis by PVX–p24, the recombinant TRV-based VIGS vector carrying a partial fragment of the endogenous *NbRAR1* was constructed (TRV–RAR1). *N. benthamiana* leaves were infiltrated with TRV–RAR1 to silence *NbRAR1* and infiltration of TRV was used as a control. At 15 dpi, qRT-PCR results confirmed the gene was indeed knocked down: the transcript level of *NbRAR1* in the first systemically TRV–RAR1-infected leaves was 42% of that in controls (Fig. 2D). Then, PVX–p24 was infiltrated into the second systemically TRV–RAR1- or TRV-infected leaves. Silencing of *NbRAR1* resulted in a 4- to 5-day delay in the necrotic response in *NbRAR1*-silenced plants (Fig. 2E). Ninety percent of *NbRAR1*-silenced plants (18 of the 20 VIGS-treated plants) showed necrosis in the PVX–p24-infiltrated patches and apical necrosis at 11–12 dpi, and 20–21 dpi, respectively, and the whole plant died at 25 dpi, compared to 7, 15, and 21 dpi, respectively, in non-silenced control plants. In addition, RT-PCR results confirmed the presence of the p24 gene in the viral progeny (Fig. 2F).

The delayed necrotic response in *NbRAR1*-silenced plants suggested that NbRAR1 is involved in the induction of systemic necrosis triggered by PVX–p24.

3.4. The region of aa 1–180 is sufficient for p24 to trigger lethal systemic necrosis in the context of PVX infection

Our previous work showed that aa region 1–188 is necessary for p24's RSS activity (Li et al., 2018). Therefore, to determine the functional region necessary for p24's pathogenicity, six deletion mutants: p24 (1–188) (containing aa 1 to 188 of p24), p24 (1–180), p24 (1–170), p24 (1–160), p24 (10–188), p24 (10–180) were expressed from the PVX vector.

As shown in Fig. 3A, mutants p24 (1–188) and p24 (1–180), like the wild-type (wt) p24 protein, were able to elicit lethal systemic necrosis. Mutants p24 (10–188), p24 (1–170), and p24 (1–160) enhanced systemic mosaic symptoms and retained the ability to induce a mild necrotic response, but failed to elicit lethal systemic necrosis. However, expression of p24 (10–180) from PVX vector totally abolished the necrotic response; instead, the plants showed the typical phenotype of PVX infection.

To further map the functional region of p24 that is required for the necrotic response, four deletion mutants—p24 (1–150), p24 (1–130), p24 (1–100), p24 (1–80)—were expressed from the PVX vector. Mutants p24 (1–150) and p24 (1–130) both enhanced systemic mosaic symptoms and retained the ability to elicit a mild necrotic response. However, p24 (1–100) and p24 (1–80) failed to elicit a necrotic response (Fig. 3A). In addition, the necrotic spots induced by p24 (10–188), p24 (1–170), p24 (1–160), p24 (1–150), and p24 (1–130) never developed to apical necrosis, and the symptoms remained unchanged for several weeks after infiltration (data not shown). The results of the agroinfiltration of plants with the above constructs are summarized in Table 1.

To determine whether the attenuated symptoms could be due to low accumulation of the mutants, we selected p24 (1–180), p24 (10–188) and p24 (10–180) as representative of mutants that can elicit lethal systemic necrosis, trigger a mild necrotic response, and fail to induce a

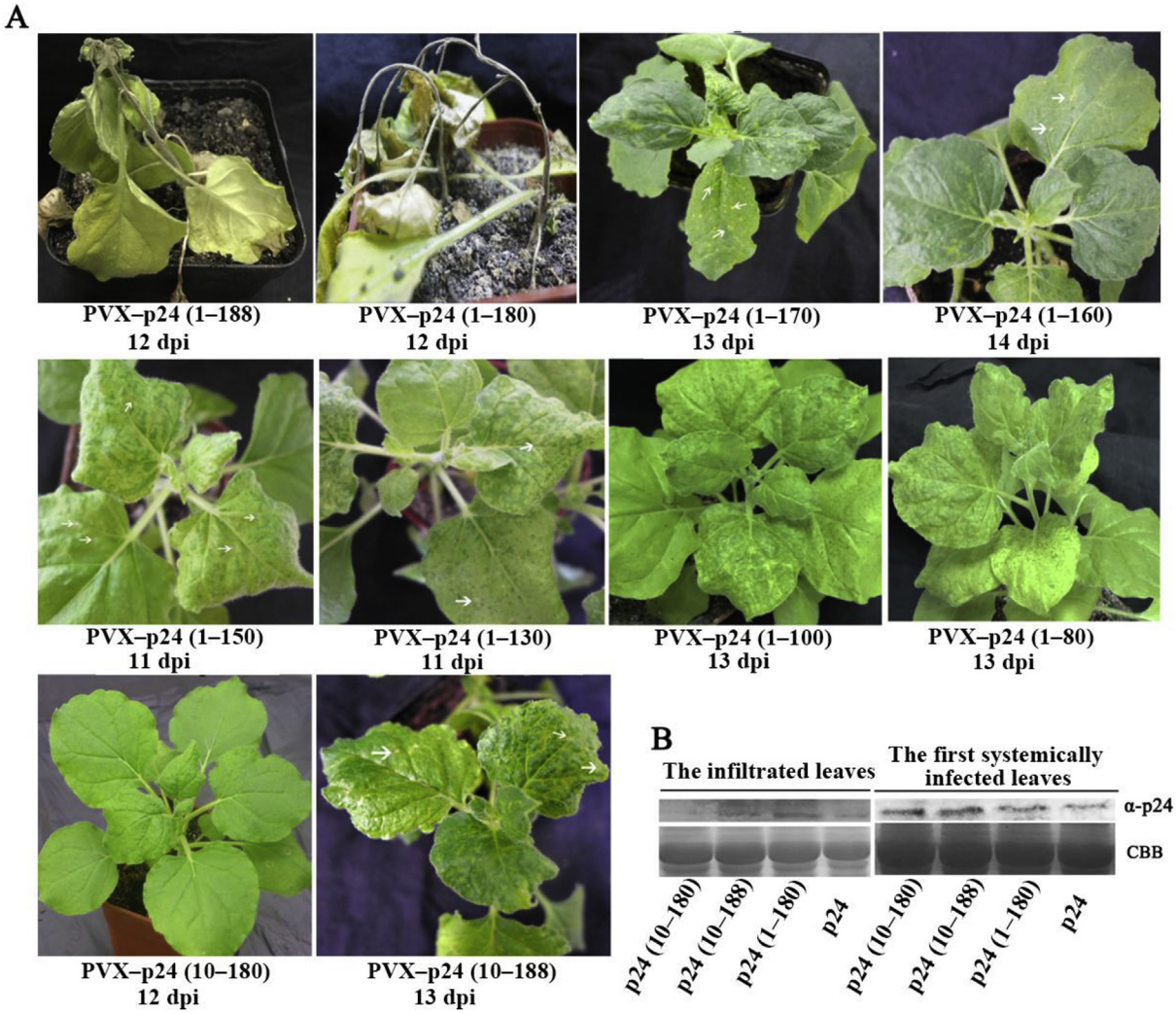

Fig. 3. Identification of regions responsible for p24's pathogenicity. (A) Phenotypes of *N. benthamiana* plants expressing p24 mutants from PVX vector. Arrows indicate necrotic spots. (B) Quantitative assessment of accumulation of wt p24 and p24 mutants by Western blot analysis using p24-specific antiserum. CBB: Coomassie brilliant blue staining served as loading control. (For interpretation of the references to color in this figure legend, the reader is referred to the Web version of this article.)

necrotic response, respectively, to detect their accumulation using an anti-p24 antiserum. The infiltrated (at 3 dpi) and first systemically infected (at 4 dpi) leaves of plants infected with each construct were harvested before necrosis was observed. Western blotting results showed that these mutants all spread systemically, and there were no obvious differences in accumulation in mutants vs. wt p24 (Fig. 3B). In addition, the other p24 deletion mutants were all accurately maintained in the viral progeny (data not shown).

These findings indicated that the region of aa 1–180 is necessary and sufficient for p24 to trigger lethal systemic necrosis in the context of a PVX expression, and that of aa 1–130 is sufficient for eliciting a mild necrotic response in *N. benthamiana* plants when expressed from a PVX vector.

3.5. Silencing-suppression-defective mutants R2A and W54A display attenuated pathogenicity

Our previous work revealed that p24 mutants R2A (alanine substitution for arginine at position 2) and W54A (alanine substitution for tryptophan at positon 54) completely lose their silencing-suppression activity (Li et al., 2018). The two mutants were expressed from PVX vector (namely PVX–R2A, and PVX–W54A) in *N. benthamiana* plants. Mutants R2A and W54A both enhanced systemic mosaic symptoms and elicited a mild necrotic response, but failed to trigger lethal systemic necrosis (Fig. 4A). The necrotic spots in PVX–R2A and PVX–W54A-infected plants never developed to apical necrosis or plant death, and the symptoms remained unchanged for several weeks (data not shown).

To determine whether mutants R2A and W54A were correctly expressed from the PVX-based vector, the infiltrated leaves at 3 dpi and the first systemically infected leaves at 4 dpi were used for western blotting analysis. No major difference in the accumulation of R2A, W54A or wt p24 was observed (Fig. 4C), suggesting that the attenuated necrotic response caused by R2A and W54A is not a result of low accumulation, but may be due to suppression inability.

These results demonstrated that the two silencing-suppression-defective mutants greatly weaken the necrotic response in *N. benthamiana* plants when expressed from PVX vector, indicating a correlation between the RNA-silencing suppression and p24 pathogenicity.

3.6. Self-interaction ability is required for p24's pathogenicity

Our previous results showed p24 mutant I35H (histidine substitution for isoleucine at position 35) retains the ability to self-interact and suppress RNA silencing, the mutant V162H/L169H/L170H (valine at position 162, and leucines at positions 169 and 170 replaced by histidines) loses self-interaction ability and has weakened RSS activity,

A

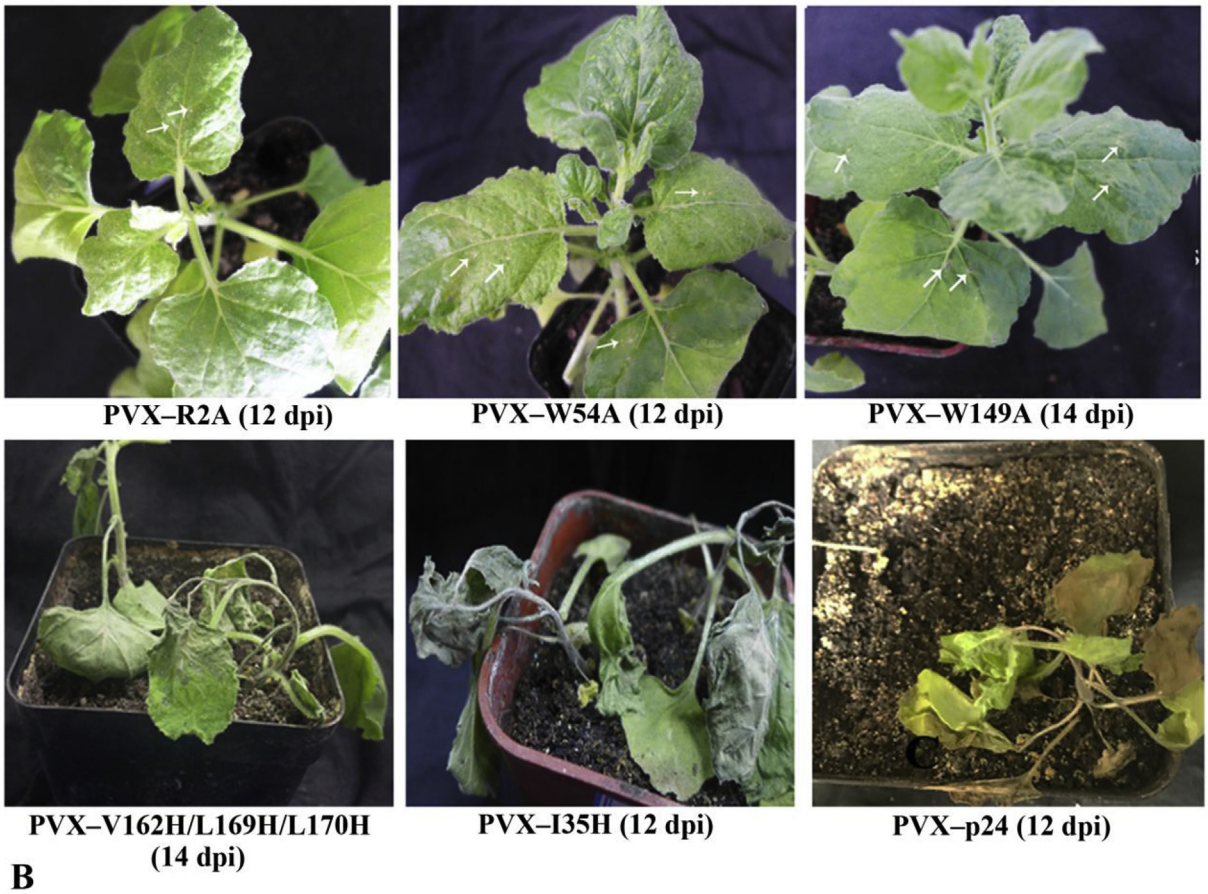

B

Construct	Phenotype	Plants exhibited phenotype/total plants
PVX–R2A	Mild necrotic response	8/9, 8/9, 7/8
PVX–W54A	Mild necrotic response	6/7, 6/7, 6/8
PVX–I35A	Systemic necrosis	6/6, 8/8, 6/6
PVX–W149A	Mild necrotic response	4/6, 5/6, 6/6
PVX–V162H/L169H/L170H	Systemic necrosis	5/5, 6/6, 6/6

C

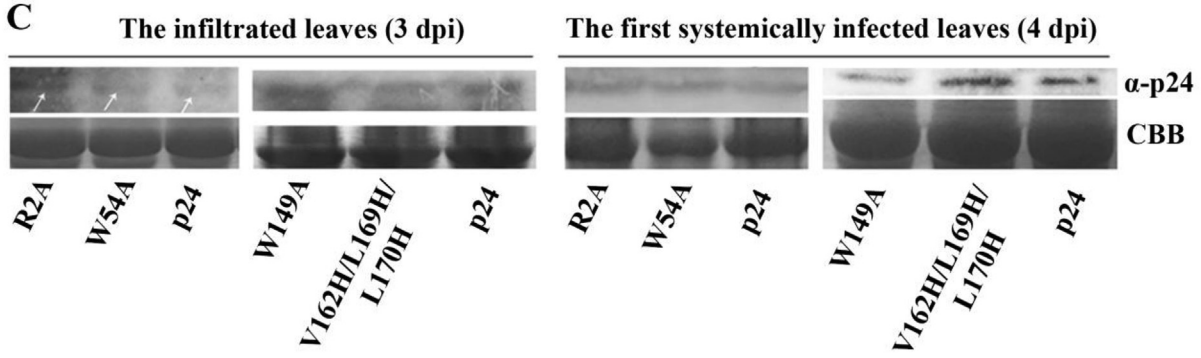

Fig. 4. Silencing-suppression-defective mutants greatly weaken the p24-mediated necrotic response. (A) Phenotypes of *N. benthamiana* plants infiltrated with PVX vector expressing wt p24 and p24 mutants. Arrows indicate necrotic spots. (B) Summary of agroinfiltration in three independent experiments. (C) Quantitative assessment of accumulation of wt p24 and p24 mutants. The infiltrated and the first systemically infected leaves were sampled at 3 and 4 dpi, respectively. Arrows indicate bands of p24. CBB: Coomassie brilliant blue staining served as loading control. (For interpretation of the references to color in this figure legend, the reader is referred to the Web version of this article.)

while the mutant W149A (alanine substitution for tryptophan at position 149) totally loses the ability to self-interact and suppress RNA silencing (Li et al., 2018). To test whether self-interaction is needed for p24's pathogenicity, mutants I35H, W149A and V162H/L169H/L170H were selected and subcloned into the PVX vector to produce PVX–I35H, PVX–W149A and PVX–V162H/L169H/L170H, respectively. Upon expression from the PVX vector, I35H or V162H/L169H/L170H elicited systemic necrosis, eventually resulting in plant death, similar to that induced by wt p24. However, the necrotic response caused by V162H/L169H/L170H was delayed by 1 or 2 days (Fig. 4A). Expression of W149A failed to elicit lethal systemic necrosis; instead, the plants only exhibited enhanced systemic mosaic symptoms with a few necrotic spots in the infiltrated and first two systemically infected leaves, and the necrotic spots never developed to apical necrosis (Fig. 4A).

We detected the accumulation levels of V162H/L169H/L170H and W149A in the infiltrated and first systemically infected leaves at 3 dpi and 4 dpi, respectively. The accumulation levels of V162H/L169H/L170H and W149A were similar to that of wt p24 (Fig. 4C).

Together, the two p24 mutants W149A and 162H/L169H/L170H previously shown to lose or retain weak RSS activity due to the lack of self-interaction displayed decreased pathogenicity, suggesting that self-interaction is also needed for p24's pathogenic activity.

4. Discussion

Global isolates of GLRaV-2 segregate into six lineages (Jarugula et al., 2010). Previous studies showed that inoculation of GLRaV-2 isolates of the PN lineage such as '94/970' (i.e. 'PN' isolate) (Goszczynski et al., 1996) and 'Nb-RC' (Lanza Volpe et al., 2015) elicit necrotic response in *N. benthamiana*. During a survey aimed at identifying the role of GLRaV-2 proteins in viral pathogenesis, the phenotype of lethal systemic necrosis was observed in *N. benthamiana* when GLRaV-2 p24 was expressed from PVX vector, but not RdRP, HSP70, CP or CPm (Fig. 1A). Furthermore, BSMV–p24 induced local necrosis covering the infiltrated patches of *N. benthamiana* plants (Fig. 1A). The symptoms were highly reproducible, since 100% of plants infected with PVX–p24 or BSMV–p24 displayed phenotypes described above. The p24 protein encoded by GLRaV-2-SD used in this study shows 96.6% and 99.6% identity with that of isolates 'PN' and 'Nb-RC', respectively, and phylogenetic analysis of p24 nucleotide sequences revealed that this isolate also belongs to the PN lineage (Fig. S1). Combined with previous research, our findings suggest that p24 plays an important role in GLRaV-2 pathogenesis.

However, the necrosis induced by expression of p24 from PVX or BSMV vector is not exactly the same with symptoms previously observed in *N. benthamiana* caused by infection of GLRaV-2 isolates belonging to PN lineage (Goszczynski et al., 1996; Lanza Volpe et al., 2015). A previous study has also reported that the induction of necrosis with a recombinant PVX expressing parts of *Grapevine chrome mosaic virus* does not reproduce symptoms from the parental virus (Fernandez et al., 1999). This may be because symptoms in *N. benthamiana* caused by GLRaV-2 infection (Goszczynski et al., 1996; Lanza Volpe et al., 2015) are result from complex interactions involving several components of the virus. Support for this notion also comes from our observation that expression of CPm or HSP70h from PVX vector elicited a few necrotic spots in *N. benthamiana* (Fig. 1).

Notably, the necrotic phenotype elicited by PVX–p24 or BSMV–p24 described here was not observed in our previous work (Li et al., 2018), where the same p24 protein was expressed from a pGD vector in agro-infiltrated *N. benthamiana* plants. The possible reason for this difference is that p24 is lower expressed by agro-infiltration in the latter case, and its low accumulation level may not be sufficient to trigger necrotic response, whereas in the PVX and BSMV systems the gene is over-expressed. However, we can't rule out the possibility that proteins of PVX or BSMV may involve in the necrosis induction.

Increased accumulation of PVX RNA has been observed in plants infected with recombinant PVX viruses expressing other viral RSSs (Deng et al., 2015; Fujita et al., 2018). However, we found that the severe disease symptoms caused by PVX–p24 are not correlated with an increase in virus titer (Fig. 1B–C), which is consistent with the previous observation reported for silencing suppressor p23 of CTV (Ruiz-Ruiz et al., 2013), the other member of the *Closterovirus* genus.

Systemic necrosis elicited by PVX–p24 in *N. benthamiana* shares HR features, such as cell death, accumulation of H_2O_2, and induction of *NbPR1* expression (Fig. 2A–C), suggesting that the phenotype is associated with the induction of plant defense pathways. Moreover, silencing of *NbRAR1*, which is known to play an essential role in many R-gene-triggered resistance responses against viruses (Liu et al., 2002; Muskett et al., 2002), resulted in a 4- to 5-day delay in the necrotic response (Fig. 2D–E), implying that *NbRAR1* is also involved in the induction of systemic necrosis triggered by PVX–p24 in *N. benthamiana* plants. In addition, we observed that BSMV–p24 was restricted to the agro-infiltrated leaves, whereas PVX–p24 spread to apical non-inoculated leaves (Fig. 1). The relative large (more than 500 bp) insert size of foreign gene may limit systemic spread of BSMV (Lee et al., 2012), but there is still another possibility that p24 may act as elicitor causing HR in *N. benthamiana* plants in the context of BSMV infection, thereby inhibiting viral systemic infection.

The pathogenicity of some viral RSSs is correlated with RSS activity (González-Jara et al., 2005; Van et al., 2002; Shiboleth et al., 2007; Wang et al., 2015). We also found that two p24 mutants—R2A and W54A—which are dysfunctional in silencing suppression possibly due to the decreased binding affinity to small interfering RNA (Li et al., 2018), produced a strong attenuating effect on viral pathogenicity (Fig. 4A), suggesting a correlation between the two activities. The p19.7 RSS from GLRaV-3 shows a variable silencing activity among phylogenetic groups (Gouveia and Nolasco, 2012), and previous studies reported that phylogenetically distinct isolates of GLRaV-2 induce different symptoms in *N. benthamiana* plants (Meng et al., 2005; Ghanem-Sabanadzovic et al., 2000; Lanza Volpe et al., 2015). Therefore, it would be interesting to investigate whether the virulence differences between phylogenetically distinct GLRaV-2 isolates are related to the variable RSS activities of p24 among phylogenetic lineages.

We also found that another two p24 mutants, W149A without RSS activity and V162H/L169H/L170H with weak suppression function (Li et al., 2018), displayed decreased pathogenicity: W149A was not able to induce lethal systemic necrosis, and V162H/L169H/L170H elicited systemic necrosis, but with a 1- to 2-day delay (Fig. 4A). The lack or weakened RSS activity of the two mutants is due to disruption of the self-interaction (Li et al., 2018). Therefore, our results indicated that self-interaction is also required for p24's pathogenicity, which is consistent with Xu et al. (2013) who found that self-interaction of 2b protein (the RSS of *Cucumber mosaic virus*) is necessary for its pathogenic activity.

The aa 1–180 region that is sufficient for p24 to elicit lethal systemic necrosis in the context of a PVX expression (Fig. 3A), is located within the aa 1–188 region which has been previously shown to be necessary for p24's RSS activity (Li et al., 2018). This suggests that aa 181–188 may play a more important role in p24 silencing suppressor function than in its pathogenicity. In addition, in contrast to the lethal systemic necrosis induced by PVX–p24 (1–180), the plants expressing p24 (10–188) or p24 (10–180) only showed enhanced systemic mosaic symptoms with a few necrotic spots in leaves or a phenotype typical of PVX infection (Fig. 3A), highlighting the importance of aa 1–9 in p24's pathogenicity.

Taken together, p24 plays an important role in GLRaV-2 pathogenesis, eliciting systemic necrosis or local necrosis in *N. benthamiana* when expressed from PVX and BSMV vectors, respectively. The systemic necrosis elicited by PVX–p24 is associated with HR characteristics, and *NbRAR1* is involved in the necrotic response. The aa 1–180 region is responsible for p24 to induce systemic necrosis when expressed from PVX vector, and both the silencing suppression and self-

interaction are required for p24's pathogenic activity.

Conflicts of interest

The authors have no conflict of interest to declare.

Authors' contributions

YC and QW conceived and designed the experiments; XW and CL performed molecular work; YX and CZ supplied the plant materials; MB performed cell death analysis and H_2O_2 detection; YX and JD performed the data analysis; YC wrote the manuscript. All authors approved the final manuscript.

Acknowledgements

We thank Prof. Andrew O. Jackson (University of California, Berkeley) and Prof. Li Daiwei (China Agricultural University) for providing the BSMV vector, and Prof. Chenggui Han (Department of Plant Pathology, China Agricultural University) for kindly providing anti-PVX CP antiserum. This work was supported by the earmarked fund for Modern Agro-Industry Technology Research System (CARS-29-bc-3) and the open funds of the Key Laboratory of Viticulture and Ennology (Ministry of Agriculture, China).

Appendix A. Supplementary data

Supplementary data to this article can be found online at https://doi.org/10.1016/j.plaphy.2019.06.033.

References

Angel, C.A., Schoelz, J.E., 2013. A survey of resistance to Tomato bushy stunt virus in the genus *Nicotiana* reveals that the hypersensitive response is triggered by one of three different viral proteins. Mol. Plant Microbe Interact. 26, 240–248. https://doi.org/10.1094/MPMI-06-12-0157-R.

Chapman, S., Kavanagh, T., Baulcombe, D., 1992. Potato virus X as a vector for gene expression in plants. Plant J. 2, 549–557. https://doi.org/10.1046/j.1365-313X.1992.t01-24-00999.x.

Chiba, M., Reed, J.C., Prokhnevsky, A.I., Chapman, E.J., Mawassi, M., Koonin, E.V., Carrington, J.C., Dolja, V.V., 2006. Diverse suppressors of RNA silencing enhance agroinfection by a viral replicon. Virology 346, 7–14. https://doi.org/10.1016/j.virol.2005.09.068.

Cuellar, W.J., Kreuze, J.F., Rajamäki, M.L., Cruzado, K.R., Untiveros, M., Valkonen, J.P.T., 2009. Elimination of antiviral defense by a viral RNase III. Proc. Natl. Acad. Sci. U.S.A. 106, 10354–10358. https://doi.org/10.1073/pnas.0806042106.

Deng, X.G., Peng, X.J., Zhu, F., Chen, Y.J., Zhu, T., Qin, S.B., Xi, D.H., Lin, H.H., 2015. A critical domain of Sweet potato chlorotic fleck virus nucleotide-binding protein (NaBp) for RNA silencing suppression, nuclear localization and viral pathogenesis. Mol. Plant Pathol. 16, 365–375. https://doi.org/10.1111/mpp.12186.

Fernandez, I., Candresse, T., Gall, O.L., Dunez, J., 1999. The 5' noncoding region of grapevine chrome mosaic nepovirus RNA-2 triggers a necrotic response on three *Nicotiana* spp. Mol. Plant Microbe Interact. 12, 337–344. https://doi.org/10.1094/MPMI.1999.12.4.337.

Fujita, N., Komatsu, K., Ayukawa, Y., Matsuo, Y., Hashimoto, M., Netsu, O., Teraoka, T., Yamaji, Y., Namba, S., Arie, T., 2018. N-terminal region of cysteine-rich protein (CRP) in carlaviruses is involved in the determination of symptom types. Mol. Plant Pathol. 19, 180–190. https://doi.org/10.1111/mpp.12513.

García, J.A., Pallás, V., 2015. Viral factors involved in plant pathogenesis. Curr. Opin. Virol. 11, 21–30. https://doi.org/10.1016/j.coviro.2015.01.001.

Ghanem-Sabanadzovic, N.A., Sabanadzovic, S., Castellano, M.A., Boscia, D., Martelli, G.P., 2000. Properties of a new isolate of grapevine leafroll associated virus 2. Vitis 39, 119–121. https://doi.org/10.1007/s001220051529.

González-Jara, P., Atencio, F.A., Martínez-García, B., Barajas, D., Tenllado, F., Díaz-Ruíz, J.R., 2005. A single amino acid mutation in the Plum pox virus helper component-proteinase gene abolishes both synergistic and RNA silencing suppression activities. Phytopathology 95, 894–901. https://doi.org/10.1094/phyto-95-0894.

Goszczynski, D.E., Kasdorf, G.G.F., Pietersen, G., van Tonder, H., 1996. *Grapevine leafroll-associated virus 2* (GLRaV-2) - mechanical transmission, purification, production and properties of Antisera detection by ELISA. S. Afr. J. Enol. Vitic. 17, 15–26. https://doi.org/10.21548/17-1-2253.

Gouveia, P., Nolasco, G., 2012. The p19.7 RNA silencing suppressor from Grapevine leafroll-associated virus 3 shows different levels of activity across phylogenetic groups. Virus Gene. 45, 333–339. https://doi.org/10.1007/s11262-012-0772-3.

Jarugula, S., Alabi, O.J., Martin, R.R., Naidu, R.A., 2010. Genetic variability of natural populations of *grapevine leafroll-associated virus* 2 in Pacific Northwest Vineyards. Phytopathology 100, 698–707. https://doi.org/10.1094/phyto-100-7-0698.

Komatsu, K., Hashimoto, M., Ozeki, J., Yamaji, Y., Maejima, K., 2010. Viral-induced systemic necrosis in plants involves both programmed cell death and the inhibition of viral multiplication, which are regulated by independent pathways. Mol. Plant Microbe Interact. 23, 283–293. https://doi.org/10.1094/mpmi-23-3-0283.

Lanza Volpe, M., Moyano, S., Lijavetzky, D., Gómez Talquenca, S., 2015. Partial molecular and biological characterization of *grapevine* leafroll-associated virus 2 isolates from Argentina. J. Plant Pathol. 97, 349–355. https://doi.org/10.4454/JPP.V97I2.002.

Lawrence, D.M., Jackson, A.O., 2001. Requirements for cell-to-cell movement of Barley stripe mosaic virus in monocot and dicot hosts. Mol. Plant Pathol. 2, 65–75. https://doi.org/10.1046/j.1364-3703.2001.00052.x.

Lee, W.S., Hammond-Kosack, K.E., Kanyuka, K., 2012. Barley stripe mosaic virus mediated tools for investigating gene function in cereal plants and their pathogens: virus-induced gene silencing, host-mediated gene silencing, and virus-mediated overexpression of heterologous protein. Plant Physiol. 160, 582–590. https://doi.org/10.1104/pp.112.203489.

Li, M.J., Zhang, J., Feng, M., Wang, X.Y., Luo, C., Wang, Q., Cheng, Y.Q., 2018. Characterization of silencing suppressor p24 of *Grapevine leafroll-associated virus* 2. Mol. Plant Pathol. 19, 355–368. https://doi.org/10.1111/mpp.12525.

Liu, Y., Schiff, M., Marathe, R., Dinesh-Kumar, S.P., 2002. Tobacco Rar1, EDS1 and NPR1/NIM1 like genes are required for N-mediated resistance to tobacco mosaic virus. Plant J. 30, 415–429. https://doi.org/10.1046/j.1365-313X.2002.01297.x.

Liu, Y.P., Peremyslov, V.V., Medina, V., Dolja, V.V., 2009. Tandem leader proteases of *Grapevine leafroll-associated virus 2*: host-specific functions in the infection cycle. Virology 383, 291–299. https://doi.org/10.1016/j.virol.2008.09.035.

Liu, Q., Guo, R., Li, M., Feng, M., Wang, X.Y., Wang, Q., Cheng, Y.Q., 2016a. Critical regions and residues for self-interaction of *grapevine leafroll-associated virus* 2 protein p24. Virus Res. 220, 57–63. https://doi.org/10.1016/j.virusres.2016.04.010.

Liu, Z.Q., Liu, Y.Y., Shi, L.P., Yang, S., Shen, L., Yu, H.X., Wang, R.Z., 2016b. SGT1 is required in PcINF1/SRC2-1 induced pepper defense response by interacting with SRC2-1. Sci. Rep. 6, 21651–21658. https://doi.org/10.1038/srep21651.

Liu, Z., Li, X., Sun, F., Zhou, T., Zhou, Y., 2017. Overexpression of OsCIPK30 enhances plant tolerance to rice stripe virus. Front. Microbiol. 8, 2322. https://doi.org/10.3389/fmicb.2017.02322.

Mandadi, K.K., Scholthof, K.B.G., 2013. Plant immune responses against viruses: how does a virus cause disease? Plant Cell 25, 1489–1505. https://doi.org/10.1105/tpc.113.111658.

Meng, B., Li, C., Goszczynski, D.E., Gonsalves, D., 2005. Genome sequences and structures of two biologically distinct strains of *grapevine leafroll-associated virus 2* and sequence analysis. Virus Gene. 31, 31–34. https://doi.org/10.1007/s11262-004-2197-0.

Muskett, P.R., Kahn, K., Austin, M.J., Moisan, L.J., Sadanandom, A., Shirasu, K., Jones, J.D., Parker, J.E., 2002. Arabidopsis *RAR1* exerts rate-limiting control of R gene-mediated defenses against multiple pathogens. Plant Cell 14, 979–992. https://doi.org/10.1105/tpc.001040.

Mubin, M., Amin, I., Amrao, L., Briddon, R.W., Mansoor, S., 2010. The hypersensitive response induced by the V2 protein of a monopartite begomovirus is countered by the C2 protein. Mol. Plant Pathol. 11, 245–254. https://doi.org/10.1111/j.1364-3703.2009.00601.x.

Naidu, R.A., Maree, H.J., Burger, J.T., 2015. Grapevine leafroll disease and associated viruses: a unique pathosystem. Annu. Rev. Phytopathol. 53, 613–634. https://doi.org/10.1146/annurev-phyto-102313-045946.

Pfaffl, M.W., 2001. A new mathematical model for relative quantification in real-time RT-PCR. Nucleic Acids Res. 29, 2002–2007. https://doi.org/10.1093/nar/29.9.e45.

Pruss, G., Ge, X., Shi, M.X., Carrington, J.C., Vance, V.B., 1997. Plant viral synergism: the potyviral genome encodes a broad range pathogenicity enhancer that transactivates replication of the heterologous viruses. Plant Cell 9, 859–868. https://doi.org/10.1016/S0920-9964(00)90973-3.

Ruiz-Ruiz, S., Soler, N., Sánchez-Navarro, J., Fagoaga, C., López, C., Navarro, L., Moreno, P., Peña, L., Flores, R., 2013. Citrus tristeza virus p23: determinants for nucleolar localization and their influence on suppression of RNA silencing and pathogenesis. Mol. Plant Microbe Interact. 26, 306–318. https://doi.org/10.1094/MPMI-08-12-0201-R.

Shiboleth, Y.M., Haronsky, E., Leibman, D., Arazi, T., Wassenegger, M., Whitham, S.A., Gaba, V., Gal-On, A., 2007. The conserved FRNK boxin HC-Pro, a plant viral suppressor of gene silencing, is required for small RNA binding and mediates symptom development. J. Virol. 81, 13135–13148. https://doi.org/10.1128/JVI.01031-07.

Scholthof, H.B., Scholthof, K.B.G., Jackson, A.O., 1995. Identification of Tomato bushy stunt virus host-specific symptom determinants by expression of individual genes from a Potato virus X vector. Plant Cell 7 1157–1117. https://doi.org/10.1105/tpc.7.8.1157.

Siddiqui, S.A., Valkonen, J.P., Rajamäki, M.L., Lehto, K., 2011. The 2b silencing suppressor of a mild strain of cucumber mosaic virus alone is sufficient for synergistic interaction with tobacco mosaic virus and induction of severe leaf malformation in 2b-transgenic tobacco plants. Mol. Plant Microbe Interact. 24, 685–693. https://doi.org/10.1094/MPMI-12-10-0290.

Tai, Y.S., Bragg, J., Meinhardt, S.W., 2007. Functional characterization of ToxA and molecular identification of its intracellular targeting protein in wheat. Am. J. Plant Physiol. 2, 76–89. https://doi.org/10.3923/ajpp.2007.76.89.

Van, W.R., Dong, X., Liu, H., Tien, P., Stanley, J., Hong, Y., 2002. Mutation of three cysteine residues in Tomato yellow leafcurl virus-China C2 protein causes dysfunction in pathogenesis and post transcriptional gene-silencing suppression. Mol. Plant Microbe Interact. 15, 203–208. https://doi.org/10.1094/mpmi.2002.15.3.203.

Wang, K.D., Empleo, R., Nguyen, T.T., Moffett, P., Sacco, M.A., 2015. Elicitation of hypersensitive responses in *Nicotiana glutinosa* by the suppressor of RNA silencing proteinP0 from poleroviruses. Mol. Plant Pathol. 16, 435–448. https://doi.org/10.1111/mpp.12201.

Wang, M.B., Masuta, C., Smith, N.A., Shimura, H., 2012. RNA silencing and plant viral diseases. Mol. Plant Microbe Interact. 25, 1275–1285. https://doi.org/10.1094/mpmi-04-12-0093-cr.

Xu, A., Zhao, Z., Chen, W., Zhang, H., Liao, Q., Chen, J., Du, Z., 2013. Self-interaction of the cucumber mosaic virus 2b protein plays a vital role in the suppression of RNA silencing and the induction of viral symptoms. Mol. Plant Pathol. 14, 803–812. https://doi.org/10.1111/mpp.12051.